

BEAM OPTICS DESIGN ON A NEW INJECTION SCHEME FOR THE UNIVERSITY OF MARYLAND ELECTRON RING (UMER)*

H. Li†, R.A. Kishek, S. Bernal, T. Godlove, M. Walter, P.G. O'Shea, M. Reiser
 Institute for Research in Electronics and Applied Physics, University of Maryland,
 College Park, MD 20742

Abstract

A new optics design for beam injection into the University of Maryland Electron Ring (UMER) is proposed for multi-turn operations. We review the previous method where two pulsed and physically overlapped Panofsky quadrupoles (one is centered on the injector and the other is centered on the ring) are employed. The new design with only one DC quadrupole reduces both the mechanical and electrical complexities. The DC quadrupole is located symmetrically relative to the injector ($+10^\circ$) and the ring (-10°). The beam's centroid motion as well as space-charge-dominated beam matching is studied to evaluate the new design. Some relevant beam issues such as stability and experimental considerations are also discussed for the multi-turn operations.

INTRODUCTION

The biggest challenge for the completion of the University of Maryland Electron Ring (UMER) [1] is the design of the beam optics for the injector region. This includes several quadrupoles and dipoles in a very stringent space. We had planned initially to use two pulsed Panofsky quadrupoles [2] as well as a pulsed dipole. As illustrated in Figure 1, the Panofsky Quad 1 (PQ1), replacing one of the regular ring quadrupole, is centered on the ring for multi-turn operation, while Panofsky Quad 2 (PQ2) is centered on the injector to provide focusing for the injected beam. However, by using this method, complex mechanical and electrical issues arise despite the simplicity in the beam optics. First of all, the two Panofsky quads must physically overlap. Furthermore, PQ1 has to be squeezed between PQ2 and the pulsed dipole. Thus, we have two quads of slightly different sizes over a very stringent space. Secondly, one of the PQs must be switched on (off) while the other is off (on) to avoid field overlap. Since we are planning to use wire magnetic quadrupoles, the number of conductors has to be reduced to achieve the desired fast switching, which means we must make a compromise between field quality and circuit inductance. In order to overcome the disadvantages stated above, we have chosen a simpler scheme, which reduces both the mechanical and electrical

complexities, but also makes the beam optics more complicated than in the original design. As shown in Figure 2, one large DC quad is centered on the bisector of the injector legs and the ring, making $\pm 10^\circ$ angles with the pipe axes. When the injected and return beams pass through the large quadrupole with an angle and an axis-offset, the beams see a dipole field as well as a quadrupole field. The extra dipole term will be beneficial to assist the bending. In order to adjust the beam centroid exactly into the injection point, two extra short dipoles (SD1 and SD2) are required to steer the beam towards the quadrupole axis. Further, the large quadrupole must be a defocusing one horizontally so that the beam is bent outward of the injection point. We will describe here the relevant optics of beam centroid motion and envelope matching for injection of a space-charge-dominated beam.

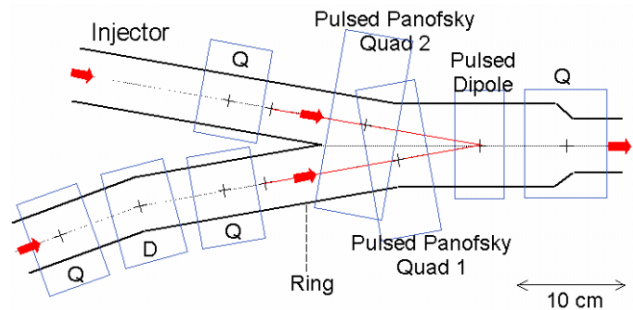


Figure 1: UMER injection design, scheme 1

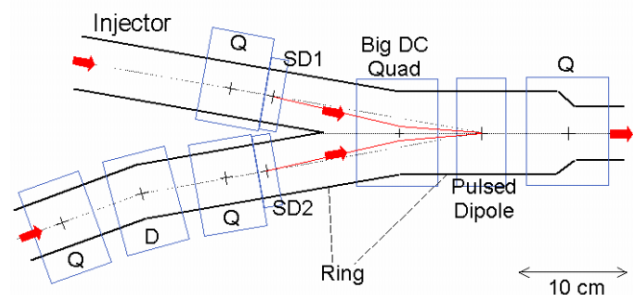


Figure 2: UMER injection design, scheme 2

BEAM CENTROID CONTROL

The deflection angle by SD1 must be precisely calculated so the beam centroid can move along the pipe

* Research supported by the U.S. Department of Energy.

† lihui@eng.umd.edu

axis after passing through the injection dipole. We have derived a first order solution for the simplified model shown in Figure 3. If we assume that the short dipole and pulsed dipole are both thin lenses, and the big DC quad is modeled with a hard-edge gradient profile and an effective length l , the overall transfer matrix can be written as $M_d \cdot M_l \cdot M_s$, where M_s , M_d and M_l are the matrices for the drift regions s , d and the quad, respectively. The matrix analysis yields the deflection angle θ (at the short dipole), and the bending angle β (at the pulsed dipole), required for zero injection error. Equations (1) and (2) give θ and β in terms of geometrical parameters and the quadrupole strength.

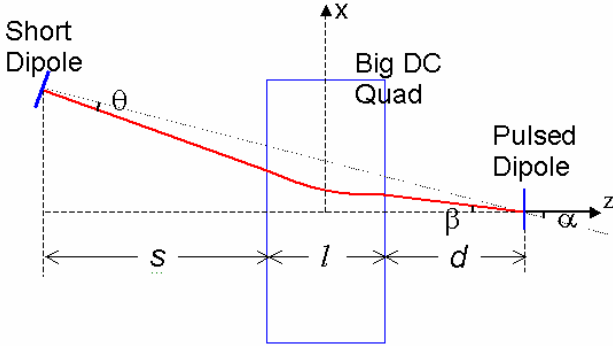


Figure 3: Simple injection model

$$\theta = \tan^{-1} \left(\frac{(a + kdb)(s + d + l)}{a(s + d) + b(1/k + ksd)} \tan \alpha \right) - \alpha, \quad (1)$$

$$\beta = \tan^{-1} \left(\frac{(s + d + l)}{a(s + d) + b(1/k + ksd)} \tan \alpha \right), \quad (2)$$

where $a = \cosh(kl)$, $b = \sinh(kl)$, $k^2 = eG/(m\gamma\beta c)$, and G is the quad field gradient. For the UMER injector, given $\alpha = 10^\circ$, $s = 6.66$ cm, $d = 4.69$ cm, $l = 6.37$ cm and $k = 11.63$ m⁻¹, we get the required deflection angle $\theta \approx 2.43^\circ$ and $\beta \approx 7.26^\circ$ from Eqs. (1) and (2).

In reality, there are several factors that lead to deviations from the above results for θ and β . First, the big DC quad has a wide fringe field; second, the short dipole and the pulsed dipole are not thin lenses either; third, UMER is often operated in the strong space-charge-dominated regime. In order to reflect all these effects, we performed a more realistic simulation with accurate 3D magnetic fields in the particle-in-cell (PIC) code WARP [3]. In this stage, we chose a typical UMER operation point: $E = 10$ keV, $I = 24$ mA, $\varepsilon = 30$ μ m, $v_0 = 7.6$ and $k/k_0 \approx 0.30$ (tune depression). The simulation yielded the exact solution $\theta \approx 2.58^\circ$ and $\beta \approx 7.23^\circ$, which agrees very well with the approximate solutions from Eqs. (1) and (2).

Another important issue besides the correct θ and β settings is the stability of the scheme. If an initial error $\Delta\theta$

is introduced by SD1, an error at the injection point will occur. The matrix analysis give the injection errors caused by errors in θ .

$$\Delta x \approx -[a(s + d) + b(1/k + ksd)] \cdot \Delta\theta, \quad (3)$$

$$\Delta\beta \approx -(a + ksb) \cdot \Delta\theta. \quad (4)$$

where Δx is the location error and $\Delta\beta$ is the angle error at the injection point. For example, if the short dipole SD1 introduces an error of 1%, the induced injection errors are about 0.1 mm and 0.05° . If the error in θ is 5%, the resultant injection errors are about 0.5mm and 0.23° . These injection errors seem small for beam transport over short distances, but it's important to understand the effect for multi-turn operation. Clearly the largest potential errors may occur at SD2 and the big quad (see Fig. 2) on the beam return.

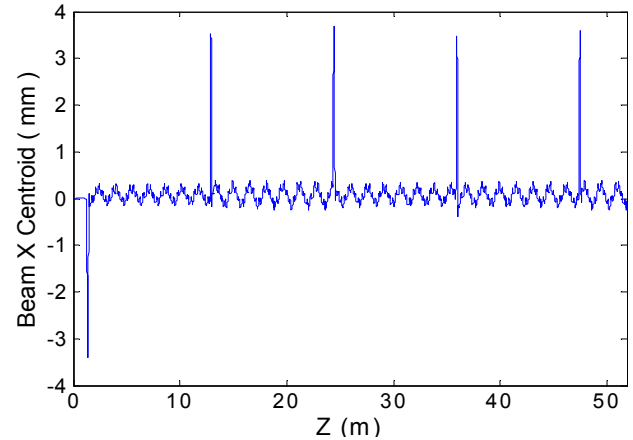


Figure 4: Beam centroids motion in 4 turns with an initial angle error 1% by SD1.

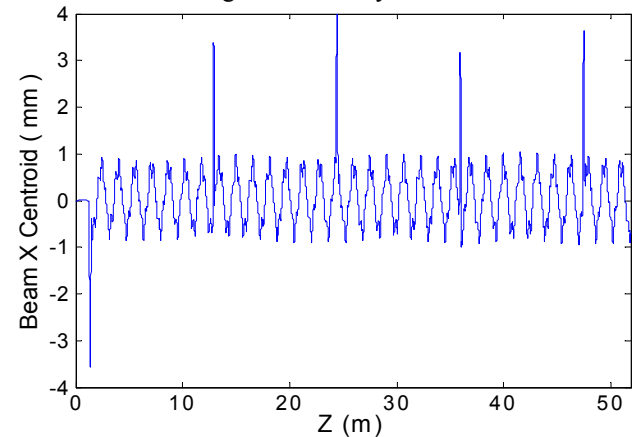


Figure 5: Beam centroids motion in 4 turns with an initial angle error 5% by SD1.

Figure 4 and 5 show the beam (x)centroid motion in 4 turns with 1% and 5% errors ($\Delta\theta/\theta$) in SD1, respectively. The bending angle by the pulsed dipole and the deflection angle by SD2 are set correctly. The beam centroid is measured relative to the reference trajectory of the ring lattice. In both Figs. 4 and 5, the first negative spike reflects the beam centroid deviation from the injector's

pipe center when passing through SD1 and the big quad. The positive spikes downstream happen exactly when the beam travels back to SD2 and the big quad in the following turns. From Fig. 4, the centroid oscillation (ripple) due to the 1% initial error is quite small. From Fig. 5, the centroid oscillations due to the 5% initial error do not grow in the following turns. The centroid ripples within 1 mm, which may be corrected with additional steering.

The mechanical design of the new injection scheme has been completed [4]. Since the magnet fields involved are small, we also need the means to balance the vertical component of the Earth's field. Equations (1) and (2) will be our starting point or guideline for future experiments. Refinements should be possible by changing the strengths of SD1 and pulsed dipole iteratively to reduce the injection errors, using a similar procedure as in the simulation. The injection errors (Δx , $\Delta\beta$) can be measured with the beam-position monitor (BPM) in the first diagnostic chamber in the ring.

BEAM MATCHING

Beam matching is an important topic besides the centroid control. The new injection scheme makes the optics design of the matching section more difficult than before. The reasons can be summarized as follows: (I) the beam will experience a changing quadrupole gradient (though the changes are small) through the big quad because of the curved trajectory. (II) The integrated field gradients along the beam trajectory for the x and y directions will be slightly different. This introduces a small asymmetry in the focusing. (III) The big quad has a much larger effective length and longer fringe fields than the regular ring quadrupoles, which impair the periodic FODO structure around the injection region. Despite these drawbacks, we can still work on a solution with the envelope sizes and slopes to do rms envelope matching. Unfortunately, we could not use the KV envelope equations to solve this problem because of the difficulties to build an accurate quadrupole model along the curved trajectory. We chose the same PIC code beam parameters as in the previous section. The beam matching is performed by varying the quadrupole strengths in the injector and observing the rms beam sizes and slopes (x , y , x' , y') at a specific location in the periodic lattice after the injection region, where the desired beam sizes and slopes are known. The result is plotted in Figure 6 for the injector region and the first half turn. The beam displays a slight mismatch ($\sim 0.5\text{mm}$) that does not grow for the following turns (not shown in the figure). It is an acceptable result considering the above effects. In the bottom part of Fig. 6, we also plotted the corresponding beam centroid motion. The negative spike occurs around the injection region, while the small ripples downstream correspond to effects from the ring bending dipoles.

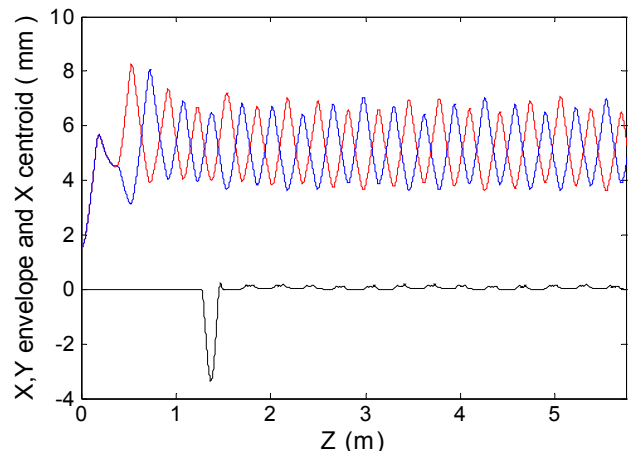


Figure 6: X-Y rms envelopes and X centroid. Solid line: x-y envelope; bottom line: x-centroid.

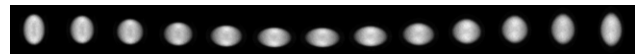


Figure 7: Simulated beam cross sections for evolution through the injection region.

Figure 7 shows the evolution of a matched beam through the injection region, starting 12 cm upstream of the large DC quad. The picture in the middle represents the beam at the center of the large DC quad. The beam centroid shift is clearly observed.

CONCLUSIONS

We have presented calculations and simulations for a new injection scheme for multi-turn operation in the University of Maryland electron Ring (UMER). The great advantage of the new scheme lies in its simplicity both mechanically and electrically: one large DC quadrupole is used instead of the two pulsed quads of the original design. In studying the beam optics, we have developed a simple model to calculate the deflection angles of the involved magnets, which can be used as the starting point for the experiments. We have also tested the stability of the system and found it to be acceptable. Furthermore, beam matching calculations with the new elements show slight mismatches that can be reduced by refinements in the design of the injection quad.

We would like to thank Tom Shea who gave us the initial idea for the injection scheme.

REFERENCES

- [1] P.G. O'Shea et al, Experiments with space-charge-dominated beams for heavy ion fusion applications, *Laser and Particle Beams*, 20, 599-602, 2002.
- [2] Y. Li, et al, Design, Simulation And Test of Pulsed Panofsky Quadrupoles, 1999 Particle Accelerator Conference (PAC'99), New York City, NY, 1999.
- [3] D.P. Grote, et al, *Fus. Eng. & Des.* 32-33, 193-200, 1996.
- [4] M. Walter et al, Electro-Mechanical Design for Injection in UMER, TPPB025, these proceedings.